BUTTERWORTH HEINEMANN

Analysis of implicit hyperbolic multivariable systems

Wieslaw Marszalek

Department of Mathematics, North Carolina State University, Raleigh, NC, USA

Zdzislaw W. Trzaska

Department of Electrical Engineering, Warsaw University of Technology, Warsaw, Poland

This paper deals with the coupled distributed parameter systems described by the system of partial differential equations (PDEs) with singular matrix coefficients. A basic classification of such systems is provided, and some properties of the systems are analyzed using the spectral theory of matrix polynomial pencils. This theory is used next for analysis of the transient behavior of superconducting energy storage coils. Several illustrative examples are included, and some numerical results showing the distribution of voltages and electric field stresses are presented.

Keywords: implicit systems, poles, finite differences

1. Introduction

Recently an interest has been shown in extending some results for singular lumped parameter systems to distributed parameter systems with singular matrix coefficients.[1,3] Such systems of coupled second-order partial differential equations appear in a number of practical applications.[4,5] In this paper, we are interested in a study of the distribution of electromagnetic signals along a superconducting energy storage coil, which is a major part of any superconducting magnetic energy storage (SMES) plant. The SMES is inherently very efficient and has siting requirements that are somewhat different from other technologies, such as, for example, compressed air, underground pumped hydro, or batteries. It promises to be an attractive technology for both defense and utility use. One of the important problems appearing in the design of a superconducting coil structure is a good knowledge of its electromagnetic characteristics, especially the strength of the coil insulation on the surge waves excited by energizing processes in the SMES systems. Studies of such phenomena are based on solutions of respective coupled partial differential equations (PDEs) with singular coefficients.

Unlike for the regular PDEs (coefficient matrices are nonsingular[6,8]), the understanding of the singular PDEs is much more complex and no good theory for classification of such systems exists.[9,10] Another problem is to analyze the eigenstructure of the systems using the spectral theory of matrix polynomial pencils. Next, it may be interesting to see if the usual discretization techniques (e.g., finite differences) can be used to solve the singular PDEs numerically.

This paper tries to identify and solve some of these problems using the Fourier technique of separation of the solution and properties of the resulting matrix polynomial pencils. We discuss the problems based on the two kinds of singular PDEs, which were already considered in Refs. 3 and 11. An application of the theory for calculation of the voltage and electric field stresses distribution within a superconducting coil due to quenches is presented.

2. Coupled systems of PDEs

We shall be concerned here with the analysis of the solution

$$\mathbf{u}(x, t) = \mathbf{G}(t)\mathbf{H}(x), \qquad \mathbf{G}(t) \in \mathbf{R}^{n \times n}, \qquad \mathbf{H}(x) \in \mathbf{R}^{n} \tag{1}$$

of the initial-boundary problem for

$$\mathbf{A}\frac{\partial^2 \mathbf{u}}{\partial x^2} = \mathbf{B}\frac{\partial \mathbf{u}}{\partial t} \tag{2}$$

or

$$\mathbf{A}\frac{\partial^2 \mathbf{u}}{\partial x^2} = \mathbf{B}\frac{\partial^2 \mathbf{u}}{\partial t^2} \tag{3}$$

Address reprint requests to Dr. W. Marszalek at the Department of Mathematics, North Carolina State University, Box 8205, Raleigh, NC 27695-8205, USA.

Received 11 January 1994; revised 17 December 1994; accepted 16 January 1995

Appl. Math. Modelling 1995, Vol. 19, July

655 Avenue of the Americas, New York, NY 10010

0307-904X/95/$10.00
SSDI 0307-904X(95)00013-A

both with $\mathbf{u}(0, t) = \mathbf{u}(l, t) = 0$ for $t \geq 0$, $\mathbf{u}(x, 0) = \mathbf{F}_0(x)$ for $t = 0$, and $0 \leq x \leq l$. It is also assumed that $\partial\mathbf{u}(x, 0)/\partial t = \mathbf{F}_1(x)$ is known for equation (3). Matrix $\mathbf{B}$ is singular but the pencils $\mathbf{R}(\lambda) = \mathbf{B}\lambda - \mathbf{A}$ (or $\mathbf{B}\lambda^2 - \mathbf{A}$) are regular, e.g. $|\mathbf{R}(\lambda)| \neq 0$.

It is known that the separation of variables applied to both equations (2) and (3) yields the following equation for the spatial vector $\mathbf{H}(x)$[3]

$$\frac{d\mathbf{H}^2(x)}{dx^2} + q\mathbf{H}(x) = 0 \tag{4}$$

while the respective equations for the $\mathbf{G}(t)$ are as follows

$$\mathbf{B}\frac{d\mathbf{G}(t)}{dt} + q\mathbf{A}\mathbf{G}(t) = 0 \tag{5}$$

or

$$\mathbf{B}\frac{d^2\mathbf{G}(t)}{dt^2} + q\mathbf{A}\mathbf{G}(t) = 0 \tag{6}$$

for equations (2) and (3), respectively. The q is a real constant to be determined.

Note that if $\mathbf{B}$ is singular, then both equations (5) and (6) are singular equations that were quite well explored in the literature over the last two decades. Singular systems (5) and (6) are sometimes called descriptor systems, differential algebraic equations, or semistate equations. They have found numerous applications in electrical and chemical engineering, econometry, mechanical systems with constraints, etc.

It is now natural, when analyzing equations (2) and (3), to ask whether equations (5) and (6) can be used to explain their nature. It turns out that all the information necessary to deal with classification of equations (2) and (3) is contained in equations (5) and (6), respectively. Particular choices of $\mathbf{A}$ and $\mathbf{B}$ give rise to different kinds of PDEs, even within the same form of equation, either (2) or (3). To begin with the analysis of equations (5) and (6), we first show how to classify systems (2) and (3) by using the approach presented in Ref. 20 and give some general consequences of such classification. From Ref. 7 if we decompose the matrix pair $(\mathbf{A}, \mathbf{B})$ into the Weierstrass canonnical form

$$\mathbf{A}, \mathbf{B} \rightarrow \begin{pmatrix} \mathbf{I} & 0 \\ 0 & \mathbf{N} \end{pmatrix}, \begin{pmatrix} \mathbf{J} & 0 \\ 0 & \mathbf{I} \end{pmatrix}$$

where $\mathbf{I}$ denotes a unit matrix, $\mathbf{J}$ is in Jordan cannonical form, and $\mathbf{N}$ is a nilpotent Jordan matrix, then we decompose equation (2) or (3), respectively into the so-called regular and nilpotent parts. Therefore, for $\mathbf{u} \equiv (\mathbf{u}_r, \mathbf{u}_n)'$ we have for the system (2) (equations for (3) are similar)[7]

$$\frac{\partial\mathbf{u}_r(x, t)}{\partial t} - \mathbf{J}\frac{\partial^2\mathbf{u}_r(x, t)}{\partial x^2} = 0$$

$$\mathbf{N}\frac{\partial\mathbf{u}_n(x, t)}{\partial t} - \frac{\partial^2\mathbf{u}_n(x, t)}{\partial x^2} = 0$$

Consider first the nilpotent subsystem where $\mathbf{N} = \text{diag}[\mathbf{N}_1\mathbf{N}_2 \ldots \mathbf{N}_k]$, and (see Ref. 7 for details about the dimensions of $\mathbf{N}_i$, $i = 1, 2, \ldots, k$)

$$\mathbf{N}_k = \begin{pmatrix} 0 & 1 & 0 & \cdots & 0 \\ 0 & 0 & 1 & \cdots & 0 \\ \cdots & \cdots & \cdots & \cdots & \cdots \\ 0 & 0 & 0 & \cdots & 1 \\ 0 & 0 & 0 & \cdots & 0 \end{pmatrix}$$

The last row of each subblock $\mathbf{N}_i$ shows that the corresponding equation is of parabolic type. This equation has only a trivial solution in the case of zero Dirichlet boundary conditions. The remaining equations within the block are also parabolic. This shows that the nilpotent subsystems for either equations (2) or (3) is of parabolic type. Therefore, equations (2) and (3) with singular $\mathbf{B}$ contain a parabolic subsystem corresponding to the nilpotent part of the Weierstrass decomposition of $(\mathbf{A}, \mathbf{B})$.

Analysis of the regular part of this decomposition indicates the type of the remaining equations according to classification in Ref. 7. Let's assume that we have an $n_1 \times n_1$ Jordan block $\mathbf{J}$ in the regular part of the decomposition. If we write an equivalent first-order system of size $2n_1 \times 2n_1$, then the system is classified according to the determinant of the matrix of principal part, denoted by $\mathbf{L}^p(\psi)$.[20] If $\det\mathbf{L}^p(\psi)$ has no real roots (i.e., there exists no real characteristic surfaces), then the system is of the elliptic type. Hyperbolicity (in one direction, usually denoted by η and associated with time variable) requires that $\det\mathbf{L}^p(\eta) \neq 0$, for some vector η, and $\det\mathbf{L}^p(i\psi + i\omega\eta)$ is a polynomial in ω with real roots, and $\mathbf{L}^p$ has a complete set of eigenvectors for each ψ not colinear with η.

Example 1

Consider equation (2) (respectively equation (5)) with

$$\mathbf{B} = \begin{pmatrix} 0 & 1 & 0 \\ 1 & 0 & 1 \\ 0 & 1 & 0 \end{pmatrix}, \quad \mathbf{A} = \mathbf{I}, \quad q_k = \frac{k\pi}{1}, \quad k = 1, 2, \ldots$$

It is easy to check that the cannonical form of $\mathbf{A}$, $\mathbf{B}$ is as follows

$$\mathbf{B} = \begin{pmatrix} 1 & 0 & 0 \\ 0 & 1 & 0 \\ 0 & 0 & 0 \end{pmatrix}, \qquad \mathbf{A} = \begin{pmatrix} 0 & \frac{1}{2} & 0 \\ 1 & 0 & 0 \\ 0 & 0 & 1 \end{pmatrix}$$

The third rows of the above matrices indicate a parabolic equation. The 2×2 regular subsystem when enlarged to a 4×4 first-order subsystem has the following $\mathbf{L}^p(\psi)$

$$\mathbf{L}^p(\psi) = \begin{pmatrix} i\psi_1 & -i\psi_2/2 & 0 & 0 \\ 0 & -1 & i\psi_2 & 0 \\ 0 & 0 & i\psi_1 & -i\psi_2 \\ i\psi_2 & 0 & 0 & -1 \end{pmatrix}$$

and $\det\mathbf{L}^p = -\psi_1^2 - \psi_2^4/2$. Therefore there are no real roots of $\det\mathbf{L}^p = 0$ and the regular subsystem is elliptic.

Really, if we assume that $\mathbf{u} \equiv (u_1, u_2, u_3)'$, then for $\mathbf{z} \equiv (z_1, z_2, z_3)' = (u_1 + u_3, u_2, u_1 - u_3)'$ we have

$$\frac{\partial^2 z_1}{\partial t^2} = \frac{1}{2}\frac{\partial^4 z_1}{\partial x^4}, \qquad \frac{\partial^2 z_2}{\partial t^2} = \frac{1}{2}\frac{\partial^4 z_2}{\partial x^4}, \qquad \frac{\partial^2 z_3}{\partial x^2} = 0.$$

The first two equations are elliptic, and the third equation is parabolic. A hyperbolic pencil resulting from equation (3) is given in Example 2.

3. Discretization of singular PDEs

Consider now the discrete versions of both equations (2) and (3) using the finite difference approximation. The Crank-Nicholson scheme was used to deal with equation (2) in Ref. 2, and we will concentrate here on equation (3) at the three time levels with the weight $m (0 \le m \le 1)$ as follows

$$\frac{\partial^2 \mathbf{u}}{\partial t^2} = \frac{\mathbf{u}(i, j+1) - 2\mathbf{u}(i, j) + \mathbf{u}(i, j-1)}{\Delta t^2} \tag{7}$$

$$\frac{\partial^2 \mathbf{u}}{\partial x^2} = \Lambda[m\mathbf{u}(i, j+1) + (1-2m)\mathbf{u}(i, j) + m\mathbf{u}(i, j-1)] \tag{8}$$

$$\Lambda \mathbf{u}(i, j) = \frac{\mathbf{u}(i+1, j) - 2\mathbf{u}(i, j) + \mathbf{u}(i-1, j)}{\Delta x^2} \tag{9}$$

This approximation when used for equation (3) yields the 9-point scheme shown in *Figure 1* with $r^2 = \Delta t^2/\Delta x^2$.

Now, equations (4) and (6) take the form

$$\mathbf{H}(i+1) - (2 + q/r^2)\mathbf{H}(i) + \mathbf{H}(i-1) = 0 \tag{10}$$

$$(\mathbf{B} - \mathbf{A}qm)\mathbf{G}(j+1) - [2\mathbf{B} + \mathbf{A}q(1-2m)]\mathbf{G}(j) + (\mathbf{B} - Aqm)\mathbf{G}(j-1) = 0 \tag{11}$$

For the proof that $\mathbf{u}(i, j) \equiv \mathbf{G}(j)\mathbf{H}(i)$ satisfies the difference scheme in *Figure 1* see the Appendix.

If $(\mathbf{B} - \mathbf{A}qm)$ is nonsingular, then equation (11) is a second-order matrix difference equation with initial conditions $\mathbf{G}(0)$ and $\mathbf{G}(1)$, both being $n \times n$ matrices. It can be written in the form

$$\mathbf{G}(j+1) - [2\mathbf{I} + (\mathbf{B} - \mathbf{A}qm)^{-1}\mathbf{A}q]\mathbf{G}(j) + \mathbf{G}(j-1) = 0 \tag{12}$$

If $(\mathbf{B} - \mathbf{A}qm)$ is singular, then equation (11) is a second-order singular equation $(\mathbf{E} \equiv \mathbf{B} - \mathbf{A}qm)$

$$\mathbf{EG}(j+1) - (2\mathbf{E} + \mathbf{A}q)\mathbf{G}(j) + \mathbf{EG}(j-1) = 0 \tag{13}$$

Assuming that $2\mathbf{E} + \mathbf{A}q$ (or equivalently $\mathbf{B} + \mathbf{A}q[1 - 2m]$) is nonsingular, we can use the Weierstrass cannonical form to decompose (13) into two subsystems

$$\mathbf{V}(j+1) - \mathbf{MV}(j) + \mathbf{V}(j-1) = 0 \tag{14}$$

$$\mathbf{SW}(j+1) - \mathbf{W}(j) + \mathbf{SW}(j-1) = 0 \tag{15}$$

where $\mathbf{G}(j) = \mathbf{V}(j) \oplus \mathbf{W}(j)$ and $\mathbf{S}$ is a nilpotent matrix.

The system of second-order matrix difference equations (10) and (11) plays the central role in the numerical analysis of equation (3). During the last decade, a number of numerical and analytical methods for solving the boundary value problems of second-order difference equations were derived. One of the most important new ideas in that domain is the concept of numerical triangles.[12] In the sequel we shall apply in our opinion, two of the most efficient methods to solve equations (10) and (11), namely the numerical triangle method, and the eigenvectors method, respectively.

It is worth noting that although the discretization procedure seems to be quite straightforward and the numerical schemes are not new, their application for implicit (singular) PDEs is not so obvious. Numerical integration of even simpler ODEs with algebraic constraints may lead to enormous difficulties, and usually special codes are required to deal with such systems, particularly if their index is greater than 1.[6] It is no surprise that system (3) is analyzed with zero Dirichlet boundary conditions, which shows that the solution of nilpotent part of equation (11) is trivially zero.[3] Otherwise, the singular equation (11) with other types of boundary conditions may lead to nonunique solutions with quite complicated spectral analysis. One can also refer to Refs. 6 and 7 for other problems in numerical integration of differential-algebraic equations by the BDF and IRK methods and description of the DASSL code.

3.1 *The numerical triangle method*

Following this approach, we can present the solution of equation (10) with condition $\mathbf{H}(0) = 0$ in the form

$$\mathbf{H}(i) = P_{i-1}(z)\mathbf{H}(1) \tag{16}$$

where $z = q/r^2$, and $\mathbf{H}(1)$ is an instantaneously unknown vector and

$$P_k(z) = \sum_{m=0}^{k} a_{k,m} z^m, \qquad k = 0, 1, 2, \ldots, N-1 \tag{17}$$

denotes a polynomial of degree k in z with constant coefficients $a_{k,m}$, $m = 0, 1, \ldots, k$. The coefficients $a_{k,m}$ are determined by the following recurrence rule

$$a_{k,l} = 2a_{k-1,l} + a_{k-1,l-1} - a_{k-2,l} \tag{18}$$

where $a_{k,0} = k + 1$, and $a_{k,k} = 1$.

The polynomials $P_k(z)$ fulfill the recurrence rule

$$P_k(z) = (2 + z)P_{k-1} - P_{k-2}(z) \tag{19}$$

where $P_0(z) = 1$ and $P_1(z) = 2 + z$.

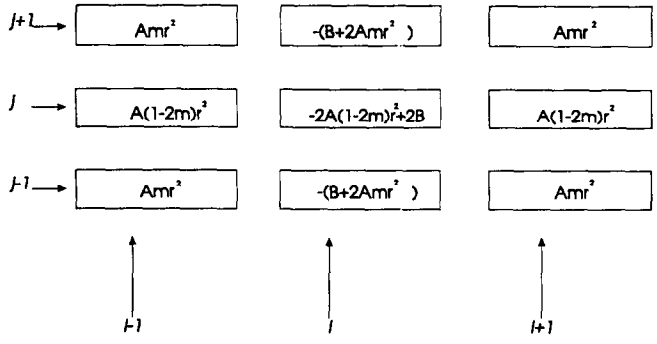

Figure 1. Schematic diagram of the 9-point difference scheme

It is easy to check that for $k = 0, 1, 2, \ldots, N-1$ all polynomials $P_k(z)$ can be evaluated from the equation

$$\begin{pmatrix} P_0 \\ P_1 \\ P_2 \\ P_3 \\ P_4 \\ P_5 \\ \vdots \\ P_{N-1} \end{pmatrix} = \begin{pmatrix} 1 & 0 & 0 & 0 & 0 & 0 & \cdots & 0 \\ 2 & 1 & 0 & 0 & 0 & 0 & \cdots & 0 \\ 3 & 4 & 1 & 0 & 0 & 0 & \cdots & 0 \\ 4 & 10 & 6 & 1 & 0 & 0 & \cdots & 0 \\ 5 & 20 & 21 & 8 & 1 & 0 & \cdots & 0 \\ 6 & 35 & 56 & 36 & 10 & 1 & \cdots & 0 \\ \vdots & \vdots & \vdots & \vdots & \vdots & \vdots & \vdots & \vdots \\ N & \cdots & \cdots & \cdots & \cdots & \cdots & \cdots & 1 \end{pmatrix} \begin{pmatrix} 1 \\ z \\ z^2 \\ z^3 \\ z^4 \\ z^5 \\ \vdots \\ z^{N-1} \end{pmatrix} \tag{20}$$

It is worth noting that the columns of the lower triangular matrix in equation (20) are identical with columns of the usual Pascal triangle[12] corresponding to the values

$$\binom{N+k}{2k+1}$$

with N being a positive integer and $k = 0, 1, 2, \ldots, N-1$.

By using equation (16) we obtain

$$\mathbf{H}(N) = P_{N-1}(z)\mathbf{H}(1) \tag{21}$$

But on the other hand the boundary condition $\mathbf{H}(N) = 0$ for $l = N\Delta x$ yields

$$P_{N-1}(z)\mathbf{H}(1) = 0 \tag{22}$$

Thus the nontrivial solution of equation (10) leads to a characteristic equation

$$P_{N-1}(z) = 0 \tag{23}$$

from which the values $q_k = z_k r^2$ of the characteristic parameter q can be computed.

It is easy to find (e.g., by applying the MATLAB package[14]) that for different N we obtain

N	$z_k = q_k/r^2$				
1	0				
2	−2.0				
3	−3.0	−1.0			
4	−3.1445	−2.0	−0.5857		
5	−3.6180	−2.6180	−1.3820	−0.3819	
6	−3.7321	−3.0	−2.0	−1.0	−0.2679
...	...	...	...	...	...	...

(24)

Thus taking into account the characteristic values of the parameter q_k, $k = 1, 2, \ldots, N-1$, we get the following particular solution for $\mathbf{H}(i)$

$$\mathbf{H}_k(i) = P_{i-1}(q_k/r^2)\mathbf{H}(1) \tag{25}$$

where $\mathbf{H}(1)$ follows from the initial conditions. In a similar way, by applying the method presented in Ref. 15 one can use a suitable algorithm for the second-order matrix difference equation (11), where $(\mathbf{B} - \mathbf{A}qm)$ is possibly singular.

3.2 *The eigenvectors method*

An alternative method for solution of equation (10) leads to the following results. It is known[5,6] that equation (10) with zero boundary conditions for $i = 0$ and $i = N$ yields a family of solutions

$$\mathbf{H}_p(i) = \sin\left(\frac{ip\pi}{N}\right)\mathbf{h}_p \tag{26}$$

where $p = 1, 2, \ldots, N-1$, and $\mathbf{h}_p$ is a constant vector. The reals q_p are found to be

$$q_p = -4r^2 \sin^2\left(\frac{p\pi}{2N}\right) \tag{27}$$

Consider now equation (12). If we denote

$$\mathbf{Q}_p \equiv -1/2(\mathbf{B} - \mathbf{A}q_p m)^{-1}\mathbf{A}q_p \tag{28}$$

then equation (14) can be written as

$$\mathbf{G}(j+1) - 2(\mathbf{I} - \mathbf{Q}_p)\mathbf{G}(j) + \mathbf{G}(j-1) = 0 \tag{29}$$

We recall the following theorem from Ref. 11.

Theorem 1

The general pencil $\mathbf{R}(\lambda) = -\mathbf{A}_0 + \lambda\mathbf{I} - \mathbf{A}_2\lambda^2$ with $\mathbf{A}_2 \neq 0$ is hyperbolic if and only if $\|\mathbf{A}_0\| \cdot \|\mathbf{A}_2\| \leq 1/4$ where $\|\cdot\|$ denotes a spectral norm.

Note that if $(\mathbf{I} - \mathbf{Q}_p)^{-1}$ exists, then applying the above condition for $\mathbf{A}_0 = \mathbf{A}_2 = \frac{1}{2}(\mathbf{I} - \mathbf{Q}_p)$ yields

$$\|\mathbf{Q}_p - \mathbf{I}\| \leq 1 \tag{30}$$

which is on the other hand equivalent to the condition that $(\mathbf{Q}_p - 2\mathbf{I}) \leq 0$. Therefore if equation (30) is satisfied, then $\mathbf{u}(i, j) \equiv \mathbf{G}(j)\mathbf{H}(i)$ is a solution of a hyperbolic system.

Example 2

Consider equation (3) with

$$\mathbf{B} = \begin{pmatrix} a^2 & 1 & 0 \\ 1 & 0 & 0 \\ 0 & 0 & 0 \end{pmatrix}, \quad \mathbf{A} = \begin{pmatrix} 1 & 0 & 0 \\ 0 & -1 & -1 \\ 0 & -1 & 0 \end{pmatrix}, \quad a \neq 0 \tag{31}$$

It can be checked that

$$\mathbf{Q}_p = \frac{1}{2q_p m^2(a^2 - q_p m)} \times \begin{pmatrix} -q_p^2 m & -q_p m & 0 \\ 0 & q_p m(a^2 - q_p m) & 0 \\ q_p m & 1 & q_p m(a^2 - q_p m) \end{pmatrix}$$

and the eigenvalues of $(\mathbf{Q}_p - \mathbf{I})$ are

$$\lambda_1 = -\frac{q_p + 2(a^2 - q_p m)}{2(a^2 - q_p m)}, \qquad \lambda_2 = \lambda_3 = -\frac{1}{2}$$

Condition (30) is now equivalent to $|\lambda_1| \leq 1$. Taking into account (27) and the fact that $0 \leq \sin^2(p\pi/2N) \leq 1$, we have

$$\frac{\Delta x^2}{\Delta t^2} \geq \frac{1 - 4m}{a^2} \tag{32}$$

Condition (32) is the well known stability condition for approximation of a scalar wave equation $a^2\partial^2 u/\partial t^2 =$

$\partial^2 u/\partial x^2$, which further simplifies to the so-called Courant condition

$$\frac{\Delta x^2}{\Delta t^2} \geq 1/a^2$$

if $m = 0$ ($1/a$ = velocity of the wave). In fact it is easy to check that from equations (3) and (31), we obtain for $\mathbf{u} = [u_1, u_2, u_3]'$ and zero boundary conditions for $x = 0$ and $x = 1$ that

$$a^2 \frac{\partial^2 u_1}{\partial t^2} = \frac{\partial^2 u_1}{\partial x^2}, \qquad \frac{\partial^2 u_2}{\partial x^2} = 0, \qquad \frac{\partial^2 u_3}{\partial x^2} = -\frac{1}{a^2}\frac{\partial^2 u_1}{\partial x^2}$$

This confirms that the system equations (3) and (31), and equivalently, the second-order matrix pencil associated with the system, is decomposed into a regular part (the wave equation for u_1), which is hyperbolic and the 2×2 nilpotent part (the last 2 equations), which is parabolic with zero solution if the zero Dirichlet boundary conditions are considered.

One can also easily check that the same result follows from the analysis of the matrix of principal part $\mathbf{L}^p$ for equation (31).

One of the methods of solving equation (29) with condition (32) is to introduce a new matrix $\mathbf{Z}_p$ such that

$$\cos \mathbf{Z}_p = \mathbf{I} - \mathbf{Q}_p, \qquad \sin \mathbf{Z}_p = [\mathbf{Q}_p(2\mathbf{I} - \mathbf{Q}_p)]^{1/2} \tag{33}$$

to get

$$\mathbf{G}_p(j) = (\cos j\mathbf{Z}_p)\mathbf{s}_p^* + (\sin j\mathbf{Z}_p)\mathbf{t}_p^* \tag{34}$$

where $\mathbf{s}_p^*$ and $\mathbf{t}_p^*$ are $n \times n$ matrices obtained from the known initial conditions and $j = 0, 1, 2, \ldots$. Then the general solution $\mathbf{u}(i, j) \equiv \mathbf{G}(j)\mathbf{H}(i)$ can be written in the form

$$\mathbf{u}(i, j) = \sum_{p=0}^{n-1} [(\cos (j\mathbf{Z}_p))\mathbf{s}_p + (\sin(j\mathbf{Z}_p))\mathbf{t}_p]\sin\left(i\frac{p\pi}{N}\right) \tag{35}$$

where $\mathbf{s}_p$ and $\mathbf{t}_p$ are $n \times 1$ vectors.

Taking into account the known initial conditions $\mathbf{F}_0(x)$ and $\mathbf{F}_1(x)$ we can expand them according to the formulas

$$\mathbf{F}_0(i\Delta x) = \sum_{p=0}^{N-1} \mathbf{f}_{0p} \sin\left(i\frac{p\pi}{N}\right) \tag{36}$$

$$\mathbf{F}_1(i\Delta x) = \sum_{p=0}^{N-1} \mathbf{f}_{1p} \sin\left(i\frac{p\pi}{N}\right) \tag{37}$$

then from equation (35) we obtain

$$\mathbf{u}(i, 0) = \sum_{p=0}^{N-1} \mathbf{s}_p \sin\left(i\frac{p\pi}{N}\right) \tag{38}$$

which together with equation (36) yields

$$\mathbf{s}_p = \mathbf{f}_{0p} \tag{39}$$

We can further use equation (33) to find

$$\frac{\mathbf{u}(i, 1) - \mathbf{u}(i, 0)}{\Delta t} = \sum_{p=0}^{N-1} [(\cos \mathbf{Z}_p - \mathbf{I})\mathbf{s}_p + (\sin \mathbf{Z}_p)\mathbf{t}_p]\left(\sin\frac{ip\pi}{N}\right)\Big/\Delta t \tag{40}$$

and

$$\mathbf{t}_p = (\sin \mathbf{Z}_p)^{-1}[(\mathbf{I} - \cos \mathbf{Z}_p)\mathbf{f}_{0p} + \Delta t\mathbf{f}_{1p}] \tag{41}$$

Thus

$$\mathbf{u}(i, j) = \sum_{p=0}^{N-1} \{[(\cos j\mathbf{Z}_p) + (\sin j\mathbf{Z}_p)(\sin \mathbf{Z}_p)^{-1}(\mathbf{I} - \cos \mathbf{Z}_p)]\mathbf{f}_{0p} + (\sin j\mathbf{Z}_p)(\sin \mathbf{Z}_p)^{-1}\Delta t\mathbf{f}_{1p}\}\sin\left(\frac{ip\pi}{N}\right) \tag{42}$$

Note that this procedure can also be used to solve equation (14). Consider now equation (15) with one elementary nilpotent block $\mathbf{N}$ of dimension $k \times k$. Because all elements of the last row of $\mathbf{N}$ are zeros, we know that all elements of the last (kth) row of $\mathbf{W}(i)$ are zeros. The elements of the $(k-1)$th row of $\mathbf{W}(i)$ are such that for $m = 1, 2, \ldots, k$ we have: $w_{k-1,m}(i) = 0$ for $i = 2, 3, \ldots,$; $w_{k-1,m}(1) = w_{k,m}(0)$; $w_{k-1,m}(0)$ is given. Going to the $(k-2)$th row of $\mathbf{W}(i)$ we have: $w_{k-2,m}(i) = 0$ for $i = 3, 4, \ldots,$; $w_{k-2,m}(2) = w_{k,m}(0)$; $w_{k-2,m}(1) = w_{k-1,m}(0)$; $w_{k-2,m}(0)$ is given. Generally $w_{k,m}(0)$ is given, $w_{k-r,m}(1) = w_{k-r+1,m}(0)$; $w_{k-r,m}(r) = w_{k,m}(0)$; $w_{k-1,m}(i) = 0$ for $i = r+1,\ r+2, \ldots$. This analysis shows that if $(\mathbf{B} - \mathbf{A}qm)$ in equation (11) is singular, then there exist constraints on the initial conditions either on $i = 0$ and $i = 1$. In other words, not all $\mathbf{u}(x, 0)$ and $d\mathbf{u}(x, 0)/dt$ may be freely chosen, as the following relation holds true

$$\Delta t \frac{\partial w_{k-r,m}}{\partial t} = w_{k-r,m}(1) - w_{k-r,m}(0) = w_{k-r+1,m}(0) - w_{k-r,m}(0)$$

for $r = 0, 1, 2, \ldots, k-1$; and $w_{k+1,m}(i) = 0$ for $i = 1, 2, \ldots, N$.

4. Spectral roots of hyperbolic pencils

It can be noticed from Section 3 that our particular interest in this paper is the hyperbolic pencils $\mathbf{R}(\lambda) = -\mathbf{A}_0 + \lambda\mathbf{I} - \mathbf{A}_2\lambda^2$ (see equations [11] and [29]), and following Ref. 11 we recall here a basic factorization theorems of such pencils.

Theorem 2

If $\|\mathbf{A}_0\| \cdot \|\mathbf{A}_2\| < 1/4$, then the pencil $\mathbf{R}(\lambda) = -\mathbf{A}_0 + \lambda\mathbf{I} - \mathbf{A}_2\lambda^2$, ($\mathbf{A}_2 \neq 0$) has a spectral root Z such that

$$\sigma(Z) = \sigma[\mathbf{R}(\lambda)] \cap D_p$$

where σ stands for spectrum, D_p is a disc $|\lambda| < \rho$, and ρ is some number such that

$$\frac{1 - \sqrt{1 - 4\|\mathbf{A}_0\| \cdot \|\mathbf{A}_2\|}}{2\|\mathbf{A}_2\|} < \rho < \frac{1 + \sqrt{1 - 4\|\mathbf{A}_0\| \cdot \|\mathbf{A}_2\|}}{2\|\mathbf{A}_2\|} \tag{43}$$

Factorization of less restrictive class of pencils is given in the following theorem (the $\ll[\gg]$ stands for uniform positivity [negativity] of the matrix).

Theorem 3

For any interval $[a, b] \subset \mathbf{R}$ and a connected and symmetric (with respect to $\mathbf{R}$) neighborhood $\mathbf{U}$ of $[a, b]$, if $\mathbf{R}(\lambda)$ is a hyperbolic pencil such that $\mathbf{R}(a) \ll 0$, $\mathbf{R}(b) \gg 0$ and $\mathbf{R}(Z) = 0$, then $\mathbf{R}(\lambda) = \mathbf{R}_+(\lambda)(\lambda\mathbf{I} - \mathbf{Z})$ where $\mathbf{R}_+(\lambda)$ is analytic and invertible in $\mathbf{U}$. Moreover, $\rho(Z) \subset (a, b)$ and $\mathbf{Z}$ is similar to a selfadjoint operator.

5. Transients in a superconducting energy storage coil

5.1 *The problem description*

In this section we will use the results of the previous sections to determine the distribution of electromagnetic field components along a superconducting coil. The superconducting coil is the heart of each SMES plant.[16] The energy storage in the superconducting coil is highly efficient because there is no conversion of energy from one form to another. The SMES has the potential of finding applications in systems with large energy storage requirements and/or rapid power changes. Such types of plants are charged and discharged through a multiphase converter, which allows it to respond within tens of milliseconds to power demands that could include a change from maximum rated charge to maximum rated discharge. This ability to respond quickly allows the SMES unit not only to function as an energy storage unit but also to perform as a spinning reserve and even to provide stability in case of disturbance outside the utility system. The components of the SMES system are shown schematically in *Figure 2*. A summary description of the technology can be found in Ref. 17.

Design of an SMES coil large enough to be practical for electric utility load leveling presents a number of significant theoretical and engineering challenges. In the process of developing of superconducting magnetic energy storage plants it is essential to understand the electromagnetic characteristics of the superconducting coil interacting with a power system through other components.[17,18] The design of the coil structure is primarily aimed for generation of a field of specified amplitude and distribution in a given volume (*Figure 3*). The SMES coils have diameters of about 70–1100 m, depending on the level of the storage energy (from 1 MWh to 5 GWh, respectively). Large coils are designed with four or more radial layers. As the life time of a SMES plant in which the coil is a major part depends on the life of the conductor and its insulation, the knowledge of voltages and electric fields within the coil must be known so that the winding distribution and the insulation is selected accordingly. Due to the ground and return capacitances and the self and mutual inductances, when the coil quenches, transient voltages and currents appear along the coil which are higher than the terminal voltage and steady-state current. The insulation must withstand these transients, specifically if the transient voltage is above the corona threshold of the conductor

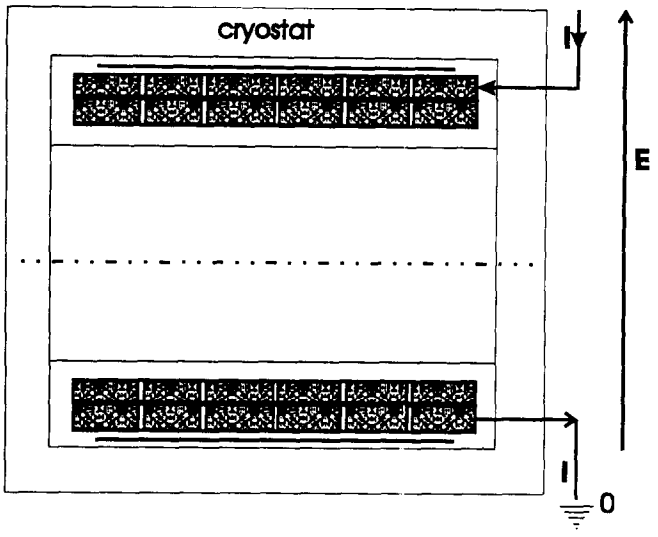

Figure 3. Diagram of a two-layer superconducting coil with one grounded end

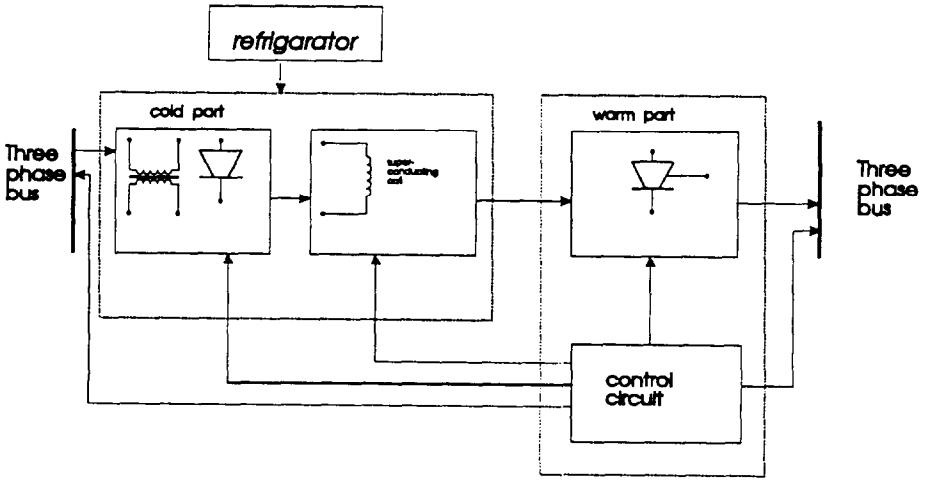

Figure 2. Diagram of a superconducting magnetic energy storage plant

insulation. Due to a quench, internal voltage surges may appear that puncture the insulation locally and may lead to partial or total coil destruction. In order to analyze the distribution of transient voltages and electric field stresses within the superconducting coil it is useful to apply the implicit PDEs but the analysis is now much more complex than in the case of classic, "hot temperature" devices.[19,26]

5.2 *Governing equations*

In the past, mathematical models of the superconducting coils were built as lumped parameter circuits with great simplifications regarding mutual impedances between turns and neglection of the residual resistances in the high temperature nature superconductors. The equivalent capacitance ladder circuit had long been used for the calculation of the initial voltage distribution along the coil. It turns out that such approximation is not valid for the analysis of the responses to a steep pulse excitation. As mentioned in Refs. 17 and 19, the capacitive circuit model of the superconducting coil winding cannot be used for analysis of the short-time switching phenomena.

Recent years have brought an increasing use of the superconducting coil for different purposes in power systems.[21–25] In many applications, the superconducting coil model is usually in the form of an ideal lumped parameter inductance. However, the main design objective in modelling any superconductive coil should be generation of a field of specific amplitude and specific distribution in a given volume. Knowledge of forces and electric fields within the coil should be accurate so that the winding distribution and insulation can be selected accordingly. The mutual coupling between the coil turns is very important to accurately model the electric field stress distributions. All of these reasons have prompted us to consider the following model of the superconducting coil.

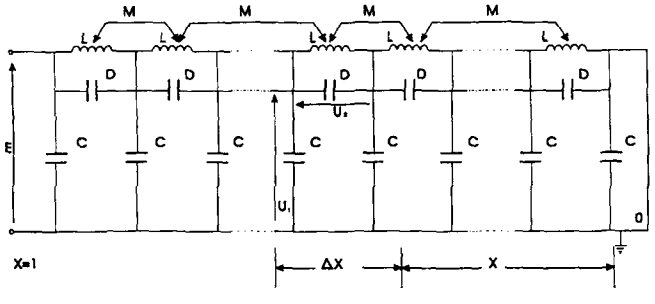

Figure 4. One-dimensional distributed parameter circuit representing the superconducting coil for surge phenomena

To estimate the internal voltage and electric field stress distribution in a superconducting coil a one-dimensional distributed structure given in *Figure 4* is used. Following the Kirchhoff laws voltages and currents in the elementary section $\Delta x \to 0$ of this structure we can establish the coil transients governing equation

$$\frac{\partial^2}{\partial x^2}\begin{pmatrix} u_1 \\ u_2 \end{pmatrix} = \begin{pmatrix} 0 & 0 \\ -LC/l^2 & L/D \end{pmatrix} \frac{\partial^2}{\partial t^2}\begin{pmatrix} u_1 \\ u_2 \end{pmatrix} + \begin{pmatrix} 0 & 1 \\ 0 & 0 \end{pmatrix}\begin{pmatrix} u_1 \\ u_2 \end{pmatrix} \tag{44}$$

where $u_1 \equiv u_1(t, x)$ and $u_2 \equiv u_2(t, x)$ denote the voltage and divergence of the electric field stress within the coil, L and M ($L \equiv M$) represent the self and mutual inductances, and C and D are the ground capacitance and between turns elastance, respectively. The parameters L, C, and D are measured per unit length of the coil conductors. The distance $x \in (0, l)$ is measured axially from the grounded end toward the terminal voltage end, where l is the length of the whole winding. The time variable $t \geq 0$ is measured from the moment of the energizing initiation in the SMES system.

The initial and boundary conditions are prescribed as follows

$$u_1(0, x) = 0, \quad u_2(0, x) = 0, \quad \frac{\partial}{\partial t} u_1(0, x) = 0, \quad \frac{\partial}{\partial t} u_2(0, x) = 0 \tag{45}$$

and

$$u_1(t, 0) = 0, \quad u_2(t, 0) = 0, \quad u_1(t, l) = E, \quad u_2(t, l) = \gamma^2 E \tag{46}$$

where E is the energizing source voltage at the input of the coil and $\gamma = (CD)^{1/2}$ is the parameter depending on the coil dimensions and material constants.

To classify equation (44) we can evaluate eigenvalues λ of the corresponding matrix pencil $\mathbf{R}(\lambda)$. Taking into account the prescribed boundary conditions in equation (46) and evaluating respective terms we obtain

$$\mathbf{R}(\lambda) = \begin{pmatrix} 0 & 0 \\ -\frac{LC}{l^2} & \frac{L}{D} \end{pmatrix}\lambda^2 - (p\pi/l)^2\begin{pmatrix} 1 & 0 \\ 0 & 1 \end{pmatrix} - \begin{pmatrix} 0 & 1 \\ 0 & 0 \end{pmatrix}$$

Thus from equation $|\mathbf{R}(\lambda)| = 0$ we get $\lambda_p = \pm(p\pi)^2 v_0 / [(p\pi)^2 + LC]^{1/2} l$, for $p = 1, 2, \ldots$ where $v_0 = (L/D)^{-1/2}$ denotes the characteristic velocity determined by the capacitance and inductance per unit length of the coil conductor.

The eigenvalues are real and of opposite sign, which yields the hyperbolic system (one can easily check the respective $\mathbf{L}^p$ for equation [44]). Note that equation (44) is slightly different than equation (3) (an additional matrix

$$\mathbf{C} \equiv \begin{pmatrix} 0 & 1 \\ 0 & 0 \end{pmatrix}$$

is included). This must also be taken into consideration to modify formulas in Section 3 and the Appendix. Such modification is done as follows. With an additional

matrix $\mathbf{C}$ in equation (44), we replace the (i,j)th node in *Figure 1* with $-2\mathbf{A}(1-2m)r^2 + 2\mathbf{B} - \mathbf{C}\Delta t^2$, and the $\mathbf{G}(j)$ coefficient in equation (11) with $2\mathbf{B} + \mathbf{A}q(1-2m) - \mathbf{C}\Delta t^2$. Appropriate terms with $\mathbf{C}$ are also added to the $\mathbf{G}(j)$ coefficients in equations (12), (13), and (28). This forces us to add $-\mathbf{C}\Delta t^2\mathbf{G}(j)\mathbf{H}(i)$ and $\mathbf{C}\Delta t^2\mathbf{G}(j)$ to the left-hand sides of equations (48) and (49) in the Appendix, respectively. The last two equations in the Appendix are still valid since appropriate cancellations of terms with $\mathbf{C}$ occur.

5.3 *Numerical results*

Applying the results given in Section 3, we can establish the solution of equation (44) with conditions (45) and (46). After some manipulations, we obtain for $p = 0, 1, 2, \ldots, N-1$

$$\mathbf{Z}_p = \Delta t(p\pi)^2(LD(p\pi)^2 + LC)\mathbf{I}$$

$$\mathbf{s}_p = \begin{pmatrix} (-1)^p(p\pi)^{-1}2CD((p\pi)^2 + CD)^{-1} \\ (-1)^{p+1}2CDp\pi N^{-2}((p\pi)^2 + CD)^{-1} \end{pmatrix}, \quad \mathbf{t}_p = 0$$

Substituting these expressions into equation (35) gives

$$\begin{pmatrix} u_1(i,j) \\ u_2(i,j) \end{pmatrix} = E\sum_{p=0}^{N-1}(-1)^p \begin{pmatrix} (p\pi)^{-1}CD((p\pi)^2 + CD) \\ -CDp\pi N^{-2}((p\pi)^2 + CD)^{-1} \end{pmatrix}^{-1}$$

$$*\cos\{j\Delta t(p\pi)^2[LD(p\pi)^2 + LC]^{-1/2}\}\sin\left(\frac{ip\pi}{N}\right)$$

For a real coil the characteristic parameters taken for computations of the distribution of the signals u_1 and u_2 are $L = 1.32$ mH/m, $C = 254$ pF/m, and $D = 0.1652$ m/pF. Computations have been performed for different number N of discretizations of the spatial variable $x = i\Delta x$, $i = 0, 1, 2, \ldots, N$ and the time variable $t = j\Delta t$, $j = 0, 1, 2, \ldots,$. The obtained results are shown in *Figures 5–7*, respectively. The whole numbers on horizontal axes in *Figures 6* and *7* correspond to the spatial variable, as follows: $0 \rightarrow 0\Delta x$, $24 \rightarrow 24\Delta x \equiv l$. All computations have been performed with using the NAP and SPICE packages.[27,28]

We see immediately that high-voltage gradients and divergences of electric field stress occur during the transition period in different parts of the coil winding. Note that the values of voltage amplitudes and divergence of electric field stress decrease rapidly as p increases. Calculation of only the first few terms of the above series is sufficient for most practical purposes.

In coils with small currents but large number of turns, the ground capacitance C is large compared with the series capacitance $1/D$, specifically if the grounded iron shell is placed within a coolant medium container and is in close proximity of the coil. Methods of reducing the product CD are to use fewer turns and to close high currents, which may solve the problem of transient voltages, but a better method is to increase the series capacitance of the coil by interlacing the turns in pancakes.

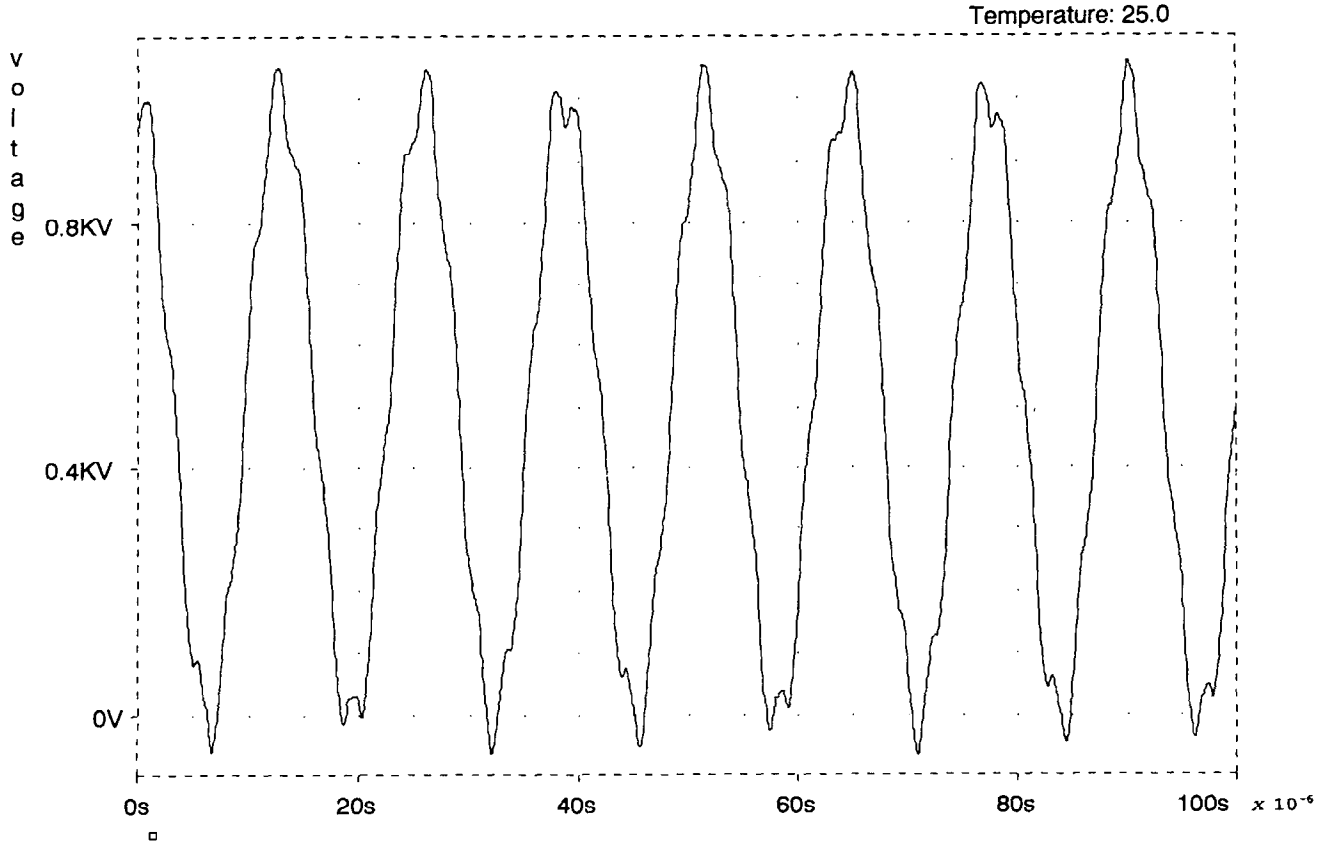

Figure 5. Transient behavior of $u_1(\frac{1}{2}, t)$, $l = 24\Delta x$, $\Delta x = 13$ m, $0 \le t \le 10^{-4}$

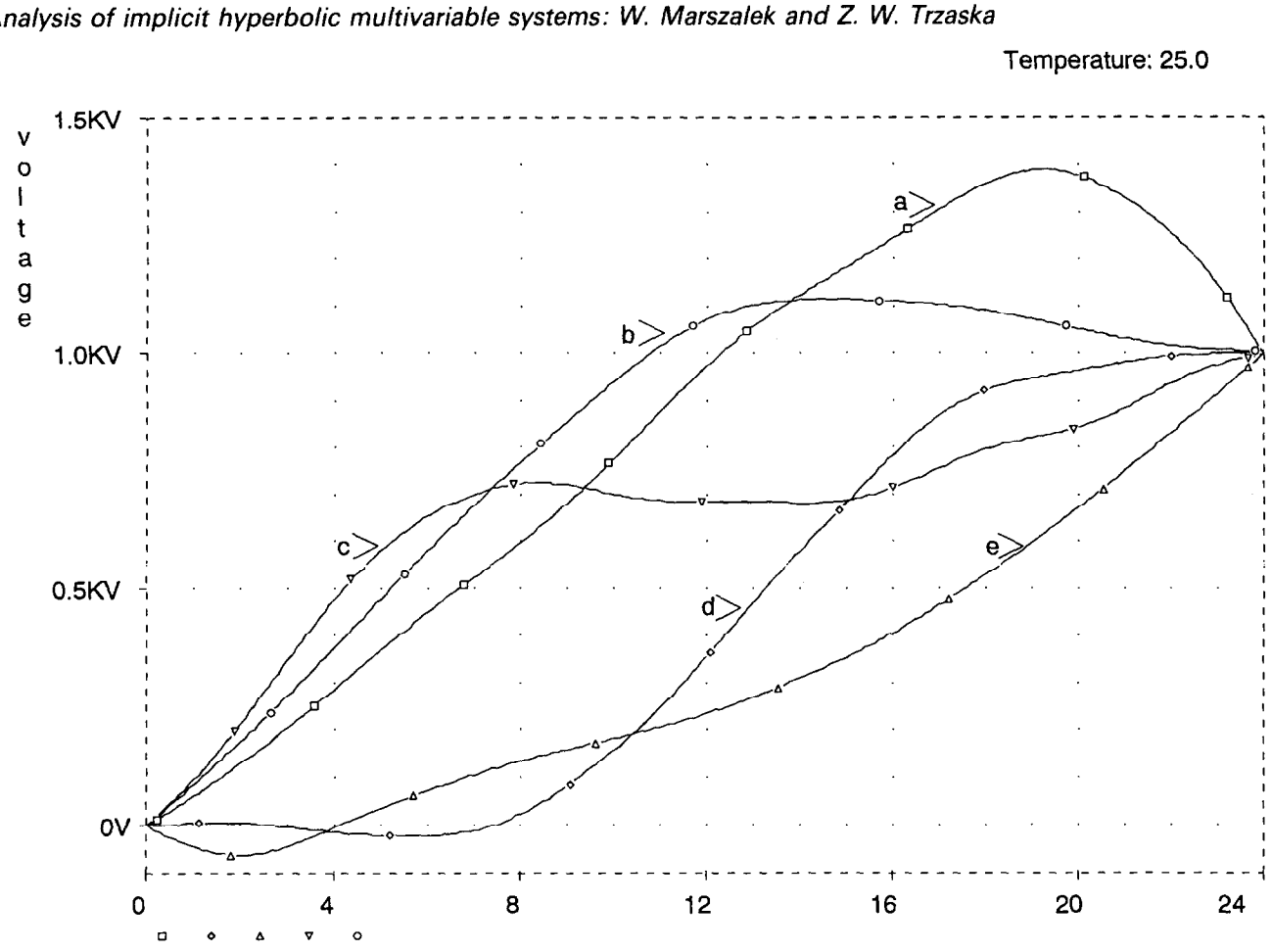

Figure 6. Distributions of $u_1(x, j\Delta t)$; $x \in [0, l]$ with $l = 24\Delta x$, $\Delta x = 13$ m, $\Delta t = 10^{-6}$ s, and (a) $j = 0$, (b) $j = 1$, (c) $j = 10$, (d) $j = 100$, (e) $j = 150$

It is hoped that these numerical observations can be verified through practical experiments. Although we do not have such comparisons thus far, some numerical results presented here seem to agree well with practical experiments in Ref. 19.

6. Conclusions

Although the focus of this paper was on hyperbolic multivariable systems and analysis of their matrix pencils, it is obvious that other systems can also be treated in a similar way. If, for example, the second-order pencil $\mathbf{R}(\lambda)$ is such that $|\mathbf{R}(\lambda)| \geq 0$ for all $\lambda \in \mathbf{R}$, then the corresponding system is said to be elliptic. It is known that a polynomial that is nonnegative on the real axis has real coefficients and even degree. The main property of an elliptic pencil is that if $\mathbf{R}(\lambda)$ is invertible for at least one $\lambda_0 \in \mathbf{R}$, then the pencil admits a factorization $\mathbf{R}(\lambda) = \mathbf{P}^*(\lambda)\mathbf{P}(\lambda)$, where $\mathbf{P}(\lambda) = \mathbf{P}_0 + \mathbf{P}_1\lambda$, $\mathbf{P}^*(\lambda) = \mathbf{P}_0^* + \mathbf{P}_1^*\lambda$ and $\mathbf{P}_1^*\mathbf{P}_1$ is the leading coefficients of a second-order pencil. It is obvious, for example, that the following pencil

$$\mathbf{R}(\lambda) = \begin{pmatrix} 1 & 0 & 0 \\ 0 & 1 & 0 \\ 0 & 0 & 0 \end{pmatrix}\lambda^2 + a^2\mathbf{I}$$

has the following factorization

$$\mathbf{P}(\lambda) = \mathbf{P}_0 + \mathbf{P}_1\lambda$$

$$= a\begin{pmatrix} 0 & 0 & 1 \\ 1 & 0 & 0 \\ 0 & 1 & 0 \end{pmatrix} + \begin{pmatrix} 0 & 0 & 0 \\ j & 0 & 0 \\ 0 & j & 0 \end{pmatrix}\lambda, \qquad (j^2 = -1)$$

Further analysis of nonhyperbolic pencils is under way.

Though considerable attention in this paper has been paid to mathematical formulations and considerations of various properties of implicit hyperbolic systems and the corresponding matrix pencils, studies presented in Section 5 have dealt with some problems concerning the distribution of electromagnetic signals within a superconducting coil. The results obtained can be used to determine the influence of some parameters of the coil, such as inductances and to ground or between-turn capacitances, respectively, on maximal values of the voltage and divergence of the electric stress during the coil energizing processes. Several studies of this concept have led to the conclusion that a strict relationship between stored energy and the strength of the superconducting coil exists.

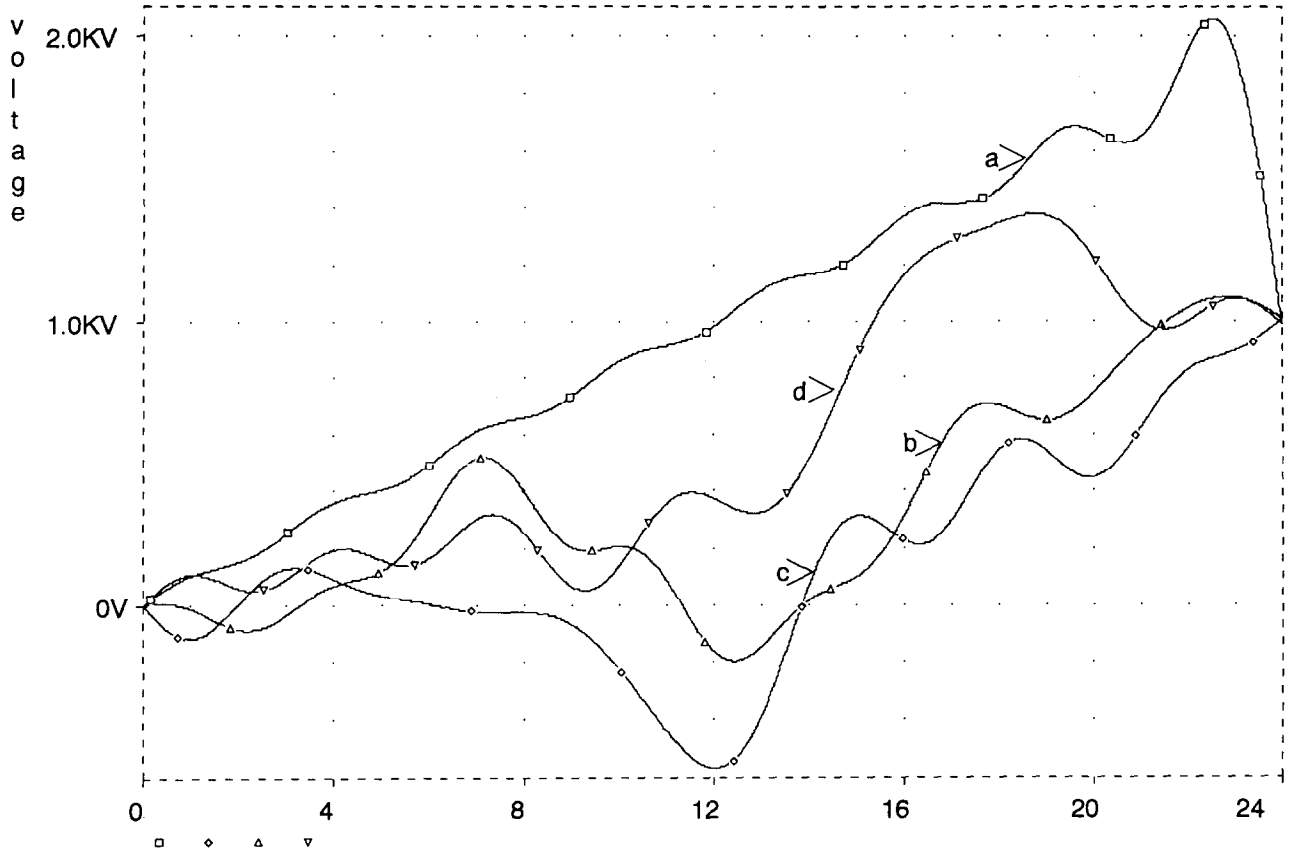

Figure 7. Distributions of $u_1(x, j\Delta t)$; $x \in [0, l]$ with $l = 24\Delta x$, $\Delta x = 13$ m, $\Delta t = 10^{-6}$ s, and (a) $j = 0$, (b) $j = 1$, (c) $j = 10$, (d) $j = 100$

Acknowledgment

The authors would like to thank one of the reviewers for his valuable comments on our preliminary version of the paper.

References

1 Solnechnyj, E. M. *Singular Systems and Their Applications in Design of Systems with Generalized Controllability* (in Russian). Nauka, Moscow, 1989
2 Jodar, L. and Legua Fernandez, M. An implicit method for the numerical solution of coupled systems of partial differential equations. *Appl. Math. Comp.* 1991, **346**, 1127–1134
3 Trzaska, Z. and Marszalek, W. *On Singular Distributed Parameter Systems.* IEE Proc. Control Theory and Applications, 1993, **140**(5), 305–208
4 Kaganov, Z. G. *Electric Distributed Parameter Systems and Ladder Networks* (in Russian). Energoatomizdat, Moscow, 1990
5 Lions, J.-L. *Controle des Systemes distribues Singuliers.* Gauthier-Villars, Paris, 1983
6 Brenan, K. E., Campbell, S. L. and Petzold, L. R. *Numerical Solution of Initial-Value Problems in Differential-Algebraic Equations.* North-Holland, New York, 1989
7 Campbell, S. L. *Singular Systems of Differential Equations.* Pitman, New York, 1980
8 Campbell, S. L. and Meyer, C. D. Jr. *Generalized Inverse of Linear Transformations.* Dover Press, New York, 1979
9 Lewis, F. L. A survey of linear singular systems. *Circuits, Systems Sig. Process* 1986, **5**(3), 3–36
10 Marszalek, W. *Structure analysis of singular systems with orthogonal functions* (in Polish). WSI Press, Series Monographs, Vol. 160, Elektryka, No. 30, Opole 1990
11 Markus, A. S. *Introduction to the Spectral Theory of Polynomial Operator Pencils.* Transl. Math. Mongr. 371(1), AMS, Providence, RI, 1988
12 Trzaska, Z. Modified numerical triangle and Fibonacci sequence. *Fibonacci Q. J.* 1994, **32**(2), 124–129
13 Brualdi, R. A. and Ryder, H. J. *Combinatorial Matrix Theory.* Cambridge Univ. Press, New York, 1991
14 *MATLAB User's Guide. Version 3.5g*, Math Works Inc., New York, 1989
15 Trzaska, Z. The Algorithm for Computing Nonmonic Second Order Multivariable Systems. *Comput. Math. Appl.* 1992, **24**(11), 17–27
16 Buckel, W. *Supraleitung. Grundlagen und Anwendungen* (in German). Physik Verlag GmbH, Weinheim, 1972
17 Foner, S. and Schwartz, B. E. (eds.) *Superconducting machines and devices.* Plenum Press, New York, 1975
18 Kusic, G. L. *Computer-aided power systems analysis.* Prentice-Hall, Englewood Cliffs, NJ, 1986
19 Brechna, H. *Superconducting Magnet Systems.* Springer-Verlag, Berlin, 1973
20 Renady, M. and Rogers, R. C. *An Introduction to Partial Differential Equations.* Springer-Verlag, New York, 1993
21 Silver, A. H. and Zimmermann, J. E. Coupled superconducting quantum oscillators. *Phys. Rev.* 1957, **158**(2), 423–425
22 Simon, R. and Smith, A. *Superconductors.* Prentice-Hall, Englewood Cliffs, NJ, 1988

23 Singh, S. K. et al. Impact of high temperature superconductors and pulsed power systems. *IEEE Trans. Magn.* 1989, **25**(2), 1787–1790
24 Chang, F.-Y. *Transient analysis of lossless transmission lines in a non-homogeneous dielectric medium.* IEEE Trans. 1970, **MIT-18**(14), 616–626
25 Sezgin, M. Magnetohydrodynamic flow in a rectangle duct. *Int. J. Num. Meth. Fluids* 1987, **7**(3), 697–718
26 Wilson, M. *Superconducting magnets.* Oxford Univ. Press, Oxford, 1983
27 Rubner-Petersen, T. *NAP2 a Nonlinear Analysis Program for Electronic Circuits, Version 2.* Techn. Univ. Denmark, Lyngby, 1973
28 Tuinenga, P. W. *SPICE: A Guide to Circuit Simulation and Analysis Using PSPICE.* Prentice-Hall, Englewood Cliffs, NJ, 1988

Appendix

From the difference scheme in *Figure 1* we have

$$\mathbf{A}mr^2\mathbf{G}(j+1)[\mathbf{H}(i+1)-2\mathbf{H}(i)+\mathbf{H}(i-1)]+\mathbf{A}(1-2m)r^2\mathbf{G}(j)[\mathbf{H}(i+1)-2\mathbf{H}(i)+\mathbf{H}(i-1)]$$
$$+\mathbf{A}mr\mathbf{G}(j-1)[\mathbf{H}(i+1)-2\mathbf{H}(i)+\mathbf{H}(i-1)]-\mathbf{B}[\mathbf{G}(j+1)-2\mathbf{G}(j)+\mathbf{G}(j-1)]\mathbf{H}(i)=0 \quad (47)$$

To prove that the left-hand side of equation (47) is equal to 0 we use the two equations following from (10) and (11)

$$\mathbf{B}[\mathbf{G}(j+1)-2\mathbf{G}(j)+\mathbf{G}(j-1)]=\mathbf{A}qm\mathbf{G}(j+1)+\mathbf{A}q(1-2m)\mathbf{G}(j)+\mathbf{A}qm\mathbf{G}(j-1) \quad (48)$$

$$\mathbf{H}(i+1)=(2+q/r^2)\mathbf{H}(i)-\mathbf{H}(i-1) \quad (49)$$

Introducing equations (48) and (49) into equation (47) we obtain

$$LHS(47)=\mathbf{A}mr\mathbf{G}(j+1)[(2+q/r^2)\mathbf{H}(i)-\mathbf{H}(i-1)-2\mathbf{H}(i)+\mathbf{H}(i-1)]$$
$$+\mathbf{A}(1-2m)r^2\mathbf{G}(j)[(2+q/r^2)\mathbf{H}(i)-\mathbf{H}(i-1)-2\mathbf{H}(i)+\mathbf{H}(i-1)]$$
$$+\mathbf{A}mr^2\mathbf{G}(j-1)[(2+q/r^2)\mathbf{H}(i)-\mathbf{H}(i-1)-2\mathbf{H}(i)+\mathbf{H}(i-1)]$$
$$-[\mathbf{A}qm\mathbf{G}(j+1)+\mathbf{A}q(1-2m)\mathbf{G}(j)+\mathbf{A}qm\mathbf{G}(j-1)]\mathbf{H}(i)$$

It is easily seen that

$$LHS(47)=[\mathbf{A}qm\mathbf{G}(j+1)+\mathbf{A}q(1-2m)\mathbf{G}(j)+\mathbf{A}qm\mathbf{G}(j-1)]\mathbf{H}(i)$$
$$-[\mathbf{A}qm\mathbf{G}(j+1)+\mathbf{A}q(1-2m)\mathbf{G}(j)+\mathbf{A}qm\mathbf{G}(j-1)]\mathbf{H}(i)=0$$